

## A continuum of $\text{InsP}_3$ -mediated elementary $\text{Ca}^{2+}$ signalling events in *Xenopus* oocytes

Xiao-Ping Sun, Nick Callamaras, Jonathan S. Marchant and Ian Parker

*Laboratory of Cellular and Molecular Neurobiology, Department of Psychobiology,  
University of California Irvine, CA 92697-4550, USA*

(Received 23 October 1997; accepted after revision 5 February 1998)

1. The elementary release events underlying inositol 1,4,5-trisphosphate ( $\text{InsP}_3$ )-mediated calcium signalling were investigated in *Xenopus* oocytes by means of high-resolution confocal linescan imaging together with flash photolysis of caged  $\text{InsP}_3$ .
2. Weak photolysis flashes evoked localized, transient calcium signals that arose at specific sites following random latencies of up to several seconds. The duration, spatial spread and amplitude of these elementary events varied widely. Event durations (at half-maximal amplitude) were distributed exponentially between about 100 and 600 ms. Fluorescence magnitudes ( $F/F_0$  of Oregon Green 488 BAPTA-1) showed a skewed distribution with a peak at about 1.5 and a tail extending as high as 3.5.
3. Individual release sites exhibited both small events (blips) and large events (puffs). The spatiotemporal distribution of calcium signals during puffs was consistent with calcium diffusion from a point source (< a few hundred nanometres), rather than with propagation of a microscopic calcium wave.
4. Estimates of the calcium flux associated with individual events were made by integrating fluorescence profiles along the scan line in three dimensions to derive the 'signal mass' at each time point. The smallest resolved events corresponded to liberation of  $< 2 \times 10^{-20}$  mol  $\text{Ca}^{2+}$ , and large events to about  $2 \times 10^{-18}$  mol  $\text{Ca}^{2+}$ . The rise of signal mass was more prolonged than that of the fluorescence intensity, suggesting that calcium liberation persists even while the fluorescence begins to decline. Rates of rise of signal mass corresponded to  $\text{Ca}^{2+}$  currents of 0.4–2.5 pA.
5. Measurements of signal mass from different events showed a continuous, exponential distribution, arising through variability in magnitude and duration of calcium flux.
6. We conclude that localized calcium transients in the oocyte represent a continuum of events involving widely varying amounts of calcium liberation, rather than falling into separate populations of 'fundamental' and 'elementary' events (blips and puffs) involving, respectively, single and multiple  $\text{InsP}_3$  receptor channels. This variability probably arises through stochastic variation in both the number of channels recruited and the duration of channel opening.

The release of calcium ions from intracellular organelles into the cytosol plays a central role in the control of diverse activities in many excitable and non-excitable cells. Inositol trisphosphate receptors ( $\text{InsP}_3\text{R}$ ) and ryanodine receptors (RyR) represent the two major types of intracellular calcium release channel, and share considerable sequence and functional homology (Berridge, 1993; Taylor & Traynor, 1995). Most notably, the opening of both of these release channels is facilitated by moderate elevations of cytosolic calcium (Fabiato, 1985; Iino, 1990; Finch, Turner & Goldin, 1991; Bezprozvanny, Watras & Ehrlich, 1991). This positive

feedback underlies the process of calcium-induced calcium release (CICR), which accounts for the generation of propagating calcium waves mediated in different cells by either  $\text{InsP}_3\text{R}$  (e.g. *Xenopus* oocytes; Lechleiter & Clapham, 1992) or by RyR (e.g. cardiac myocytes; Takamatsu & Wier, 1990). Despite the inherently regenerative nature of CICR through these channels, whole-cell calcium responses are often graded in response to stimuli, rather than showing an all-or-none characteristic (Bootman, 1994; Wier, Egan, López-López & Balke, 1994). A resolution of this paradox was provided by the discovery of 'elementary' calcium

release events; localized, transient calcium signals arising at functionally discrete release sites, which may be independently recruited or act in concert to produce calcium waves (reviewed by Lipp & Niggli, 1996*b*; Berridge, 1997). Examples of elementary calcium release events involving  $\text{InsP}_3\text{R}$  are calcium 'puffs' in *Xenopus* oocytes (Parker & Yao, 1991; Yao Choi & Parker, 1995; Parker, Choi & Yao, 1996*a*) and HeLa cells (Bootman, Niggli, Berridge & Lipp, 1997*b*), whereas analogous calcium 'sparks' in cardiac, smooth and skeletal muscle are mediated through RyR (Cheng, Lederer & Cannell, 1993; Lopéz-Lopéz, Shacklock, Balke & Wier, 1995; Nelson *et al.* 1995; Tsugorka, Rios & Blatter, 1995; Klein, Cheng, Santana, Jiang, Lederer & Schneider, 1996).

As originally described, both puffs (Yao *et al.* 1995) and sparks (Cheng *et al.* 1993) were thought to represent relatively stereotyped events. That is to say, repeated events at the same or different sites appeared to be of similar magnitude and time course, and could be considered as uniform 'building blocks' in the generation of the global cellular signal. Subsequent studies with improved resolution, however, have revealed greater complexity. Stationary-point confocal microfluorimetry allowed detection of calcium release events ('blips') in *Xenopus* oocytes that were yet smaller than the puffs (Parker & Yao, 1996) and similar blips were spatially resolved in HeLa cells by linescan imaging (Bootman *et al.* 1997*b*). In cardiac myocytes, experiments evoking calcium release by photolytic pulses of calcium led Lipp & Niggli (1996*a*) to infer the existence of calcium 'quarks' smaller than the sparks. It has been proposed that the blips and quarks represent 'fundamental' events of calcium signalling, arising through the opening of individual release channels, whereas the puffs and sparks represent 'elementary' events involving the concerted activation of several tightly clustered channels by local calcium feedback (Parker *et al.* 1996*a*; Parker & Yao, 1996; Lipp & Niggli, 1996*b*; Berridge, 1997; Bootman *et al.* 1997*b*).

Our initial discovery of calcium blips (Parker & Yao, 1996) was made using a point confocal microscope, which provided no information regarding the spatial distribution of calcium during those events. In the present paper, we have extended those studies of elementary calcium signalling events in the *Xenopus* oocyte by using a 'home-made' linescan confocal microscope with high spatial and temporal resolution to image blips and puffs evoked by photoreleased  $\text{InsP}_3$ . A major conclusion is that rather than comprising a hierarchy of stereotyped events with abrupt steps in magnitude (blips and puffs), signals evoked at a constant  $[\text{InsP}_3]$  form a continuum of events of graded size and variable time course. Blips and puffs are not, therefore, clearly distinct 'quantal' signals of uniform magnitude, but represent the opposite ends of a continuous distribution of local signals involving the release of differing amounts of calcium. In the following paper (Callamaras, Marchant, Sun & Parker, 1998) we go on to consider the progressive recruitment of elementary events by increasing concentrations of  $\text{InsP}_3$ , and their co-ordination to generate global calcium signals.

Abstracts describing this work have been presented to the Society for Neuroscience (Sun, Callamaras & Parker, 1997) and The Physiological Society (Marchant, Callamaras, Sun & Parker, 1998).

## METHODS

Experiments were done on defolliculated immature oocytes from *Xenopus laevis*. Frogs were anaesthetized by immersion in a 0.17% aqueous solution of MS-222 (3-aminobenzoic acid ethyl ester) for 15 min, and were allowed to recover after surgical removal of small pieces of ovary. Procedures for preparation of oocytes and intracellular injection were as described in Parker (1992). In brief, oocytes were loaded by intracellular microinjection 1–2 h before recording with the fluorescent calcium indicator Oregon Green 488 BAPTA-1 and with caged  $\text{InsP}_3$  (*myo*-inositol 1,4,5-trisphosphate,  $\text{P}^{4(5)}$ -1-(2-nitrophenyl) ethyl ester), to respective final intracellular concentrations of about 40  $\mu\text{M}$  and 5  $\mu\text{M}$  (assuming distribution throughout a cytosolic volume of 1  $\mu\text{l}$ ). Recordings were made at room temperature, with oocytes bathed in normal Ringer solution (composition, mM: NaCl, 120; KCl, 2;  $\text{CaCl}_2$ , 1.8; Hepes, 5; at pH  $\sim 7.2$ ). Oregon Green was obtained from Molecular Probes, Inc. (Eugene, OR, USA) and caged  $\text{InsP}_3$  from Calbiochem (San Diego, CA, USA) and Molecular Probes. All other reagents were from Sigma Chemical Co.

Confocal linescan imaging and flash photolysis of caged  $\text{InsP}_3$  were performed using systems described previously (Parker, Zang & Wier, 1996*b*; Parker, Callamaras & Wier, 1997), constructed around an Olympus IX70 inverted microscope equipped with a  $\times 40$  oil-immersion fluor objective lens (NA, 1.35). Imaging was achieved using a confocal scanner interfaced through the video port of the microscope. In brief, the 488 nm beam from a 100 mW argon ion laser (Melles Griot, Carlsbad, CA, USA) was attenuated and expanded to overfill the back aperture of the objective. A galvanometer-driven mirror (Cambridge Technology, Watertown, MA, USA) repeatedly scanned the laser spot focused in the specimen along a line 50  $\mu\text{m}$  long. Fluorescence emission was descanned by the same mirror, long-pass filtered at  $\lambda > 515$  nm and, after passing through a confocal pinhole transmitting only the central peak of the Airy disc, was focused onto an avalanche diode photon counting module (SPCM-AQ-121; EG & G Canada Ltd, Dumberry, Vaudreuil, Quebec, Canada). A separate UV system, interfaced through the epifluorescence port of the microscope, was used for flash photolysis of caged  $\text{InsP}_3$  (Callamaras & Parker, 1998). Light was derived from a continuous 75 W Xenon arc lamp, with the flash duration set by an electronically controlled shutter and the intensity varied by neutral density filter wheels. Wavelengths between about 340 and 400 nm were selected by a standard Olympus UV filter cube, and the light was focused on the oocyte as a uniform spot of about 100  $\mu\text{m}$  diameter, centered around the laser scan line.

Photon counts from the avalanche diode module were integrated during successive pixel intervals by a custom-built digital circuit and recorded on computer disc for subsequent construction of linescan images using routines written in the IDL programming language (Research Systems, Inc., Boulder, CO, USA). Unless otherwise noted, images were formed at a scan rate of 8 ms per line, with a nominal pixel size of 0.133  $\mu\text{m}$  and an integration time of 20  $\mu\text{s}$  per pixel. In some experiments a scan rate of 1.5 ms per line was used to achieve faster temporal resolution, at the expense of a shorter (5  $\mu\text{s}$ ) pixel integration time and reduced spatial resolution (0.2  $\mu\text{m}$  per pixel). The point-spread function of the confocal

system, measured using  $0.1\ \mu\text{m}$  fluorescent beads, was  $< 300\ \text{nm}$  lateral and  $< 500\ \text{nm}$  axial. All recordings were obtained with the scan line focused at the depth of the pigment granules in the oocyte (roughly  $6\ \mu\text{m}$  below the surface), where  $\text{Ins}P_3$ -sensitive release sites are concentrated (Yao *et al.* 1995). Fluorescence signals are expressed as ratios ( $F/F_0$  or  $\Delta F/F_0$ ) of the fluorescence at each pixel during a response ( $F$ ) relative to the resting fluorescence at that pixel before stimulation ( $F_0$ ). Mean values for  $F_0$  were obtained by averaging over several scan lines before the photolysis flash. Note that no change in fluorescence corresponds to  $F/F_0 = 1$  and  $\Delta F/F_0 = 0$ .

Calculation of the 'signal mass' associated with calcium release events was done using a custom routine written in IDL to integrate the one-dimensional linescan profile throughout three dimensions. Events were selected that appeared to involve calcium release from only a single site, were in sharp focus, and were well separated in time or space from other signals. The centre of the event was identified visually and, for each time point (scan line), the routine then summed the fluorescence signals ( $\Delta F/F_0$ ) along the scan line, with each value weighted by the third power of the distance of that pixel from the centre. The resulting sums were then scaled in units of  $1\Delta F/F_0 \times 10^{-15}\ \text{l}$ , representing a doubling in fluorescence throughout a volume of 1 femtolitre. Because of the third-power weighting, signal mass measurements showed greatly increasing noise and susceptibility to error from calcium originating at other sites as the integration was performed at increasing distances from the event centre. Calculations were, therefore, restricted to a limited region of sufficient width to encompass virtually all of the signal.

## RESULTS

### Linescan imaging of calcium puffs

Figure 1A illustrates our basic experimental protocol, and shows two consecutive records of  $\text{Ins}P_3$ -evoked puffs evoked along a fixed scan line by repeated, identical photolysis flashes. Successive scans in the images are stacked from left to right, so that distance along the scan line is depicted vertically, and time horizontally. A shutter blocked the laser beam for a brief period at the beginning of the records, to provide a black level and timing marker, and a flash of UV light was then delivered 300 ms after the shutter opening (indicated by the dashed lines) to photorelease  $\text{Ins}P_3$ . In this and all other images, fluorescence signals are expressed as a pseudo-ratio ( $F/F_0$ ) and are depicted by a pseudocolour scale as indicated by the colour bars. Intervals of 60 s were allowed for recovery between successive trials (Parker & Ivorra, 1990) and, in favourable cases, it was possible to obtain twenty to thirty records from a given linescan position. Because of the enormous volume of the oocyte, and the restricted area and strength of UV irradiation, consumption of caged  $\text{Ins}P_3$  was negligible during repeated flashes (Parker, 1992). All experiments in the present paper were done using photolysis flashes of a strength about 50–70% of that which just triggered calcium waves so that on average, each flash evoked a few discrete calcium release events (Callamaras *et al.* 1998). As is evident in Fig. 1A,

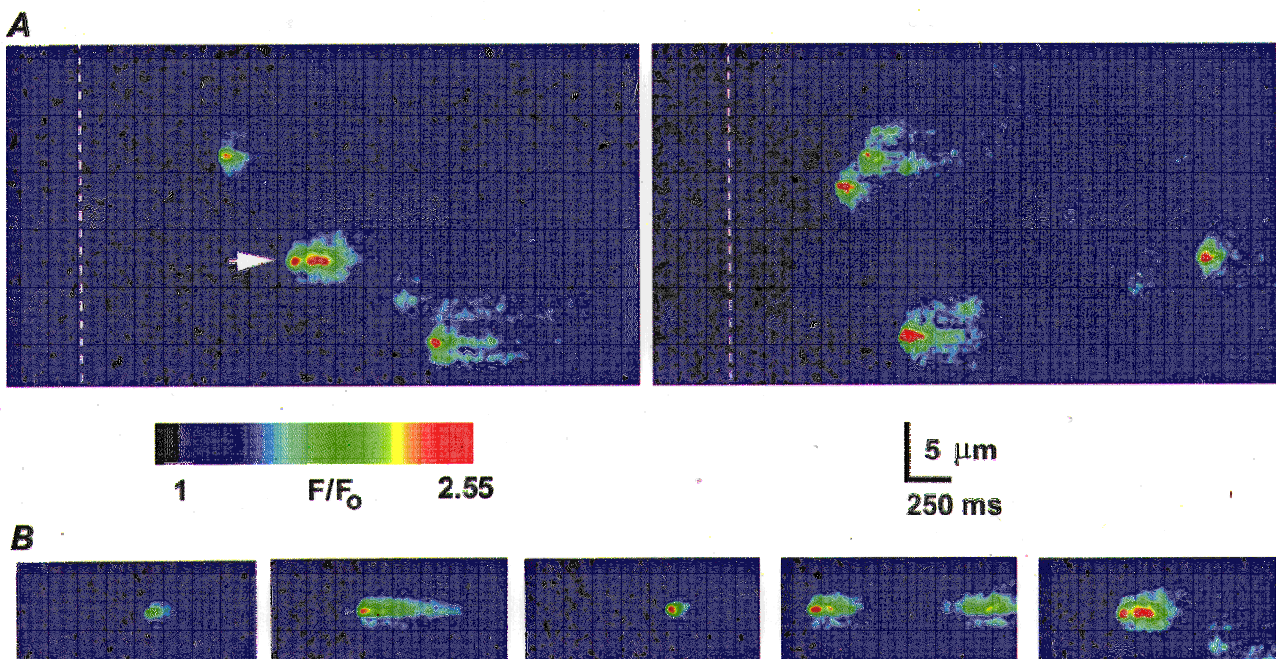


**Figure 1.** Calcium puffs evoked by photoreleased  $\text{Ins}P_3$

A, representative linescan images showing calcium puffs evoked by two successive photolysis flashes (50 ms duration) at 60 s intervals, delivered when marked by the dashed lines. B, selected examples of puffs evoked at a fixed location (site marked by arrow in A) by repeated, identical flashes, illustrating the variable durations of events generated at a given release site. Images were captured at varying times after the photolysis flashes.

puffs tended to recur at specific sites during repeated trials (example marked by arrow), but occurred after highly variable latencies.

### Variability in time course of puffs

Although puffs were initially considered to be fairly stereotypical events (Yao *et al.* 1995; Parker *et al.* 1996*a*), a more detailed examination of the records obtained with improved resolution revealed considerable variability in their time course. For example, Fig. 1*B* illustrates linescan images of several puffs arising at the same release site and Fig. 2*A* shows superimposed time courses of some of these events. Despite being evoked by identical photolysis flashes, the durations of the puffs varied almost 10-fold, though it is not yet clear whether the longer events represent a sustained calcium liberation or a rapid burst of several unresolved puffs. The variability in kinetics of the microscopic puffs stands in marked contrast to the highly consistent time course of repetitive, macroscopic calcium waves evoked during the sustained photorelease of InsP<sub>3</sub> (Fig. 2*B*).

To quantify puff duration, we measured the times for which the fluorescence intensity at a puff site remained above one-half of the maximal value. Figure 2*C* shows the distribution of half-peak times from eighty-one events. Puffs showed minimum durations of roughly 100–150 ms, presumably corresponding to the minimum durations of calcium liberation together with the time required for diffusion of

calcium away from the release site and its resequestration. Many events had appreciably longer durations, however, suggesting a more sustained duration of calcium liberation. Thus, termination of calcium release during puffs may be subject to stochastic variability and consistent with this, the distribution of puff durations in Fig. 2*C* showed a roughly exponential decline in numbers of events of progressively increasing duration.

### Puffs and blips

In addition to calcium puffs, linescan images also showed many events of lower peak amplitude and more restricted spatial spread (Fig. 3*A*). These latter signals presumably correspond to the calcium blips we had previously recorded by stationary point microfluorimetry (Parker & Yao, 1996), and which have also been imaged by confocal linescanning in HeLa cells (Bootman *et al.* 1997*b*). As illustrated in Fig. 3*A*, blips occurred at sites that also showed puffs, and were observed as both isolated events or, more rarely, were seen closely preceding and possibly triggering puffs.

Images in Fig. 3*B* were obtained by averaging selected blips ( $n = 5$ ) and puffs ( $n = 4$ ) after aligning the original images in space and time relative to the peak fluorescence signal in each case. The kinetics of the averaged blip were more rapid than those of the puff (Fig. 4*A*), with respective durations at half-peak amplitudes of 96 and 208 ms, and the spatial spread of calcium during the blip was more restricted (widths

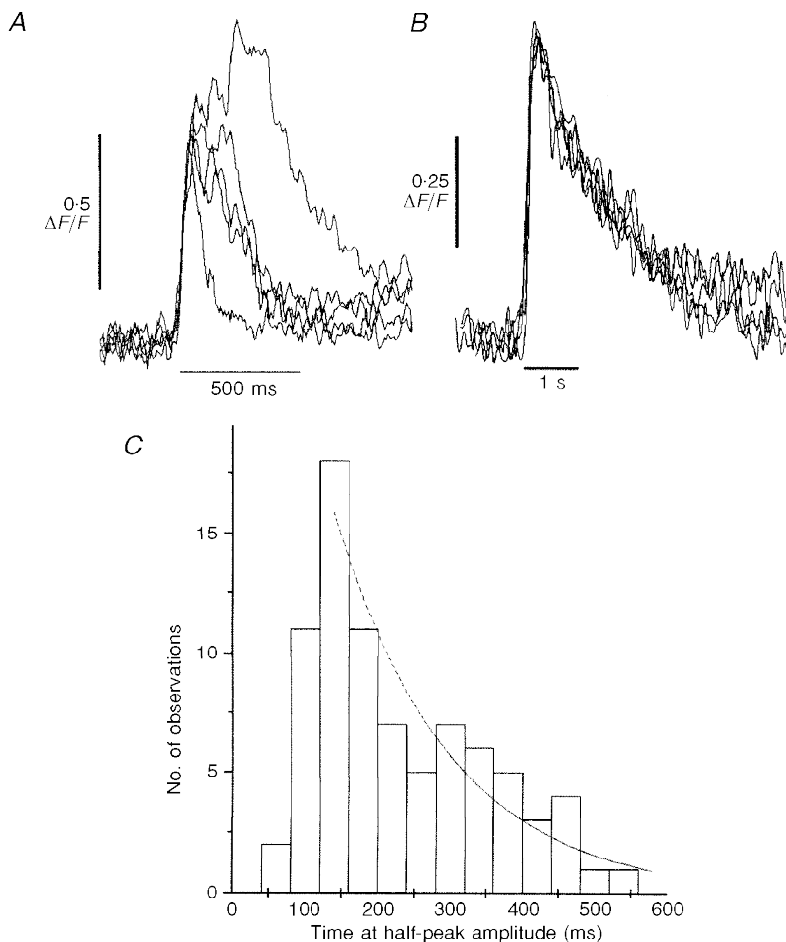


**Figure 2. Puffs show wide variability in their durations, in contrast to the constancy in calcium wave kinetics**

*A*, superimposed records showing kinetics of puffs evoked at a single site by repeated, identical photolysis flashes. Traces show fluorescence ratios ( $\Delta F/F_0$ ) measured from a 3 pixel ( $0.4 \mu\text{m}$ ) region centered on the puff site, and are aligned by their rising phases. Same experiment as Fig. 1*B*.

*B*, superimposed traces showing kinetics of repetitive calcium waves. Signals show fluorescence monitored with the low-affinity indicator Calcium Green-5N, and were monitored from  $1 \mu\text{m}$  wide regions of linescan images. Repetitive waves were induced by sustained photorelease of InsP<sub>3</sub> by prolonged (minutes) exposure to low-intensity UV light. *C*, distribution of puff durations. Measurements from traces like those in *A* were obtained of the times for which the fluorescence signal exceeded one-half of the peak amplitude during each puff. Data are from 81 sharply focused events, all recorded in the animal hemisphere.

at half-maximal amplitude of 1.5 and 4.1 μm, respectively). These findings, together with the localization of blips at puff sites (Fig. 3*A* and see later), indicate that sharply imaged blips arise through release of small amounts of calcium at sites focally imaged by the laser line, rather than arising artifactually through diffusive spread of calcium liberated during puffs distal (laterally or axially) to the scan line. Additional evidence against the latter possibility is that

images of puffs evoked at a given location became progressively more faint and diffuse when the microscope was deliberately defocused away from the release site, rather than appearing more sharply defined (not shown). Furthermore, the time course of fluorescence monitored at a distance (2 μm) from the centre of the puff where the peak amplitude matched that of the blip was slightly slower than the focal puff signal and much slower than the blip (Fig. 4*A*, inset).

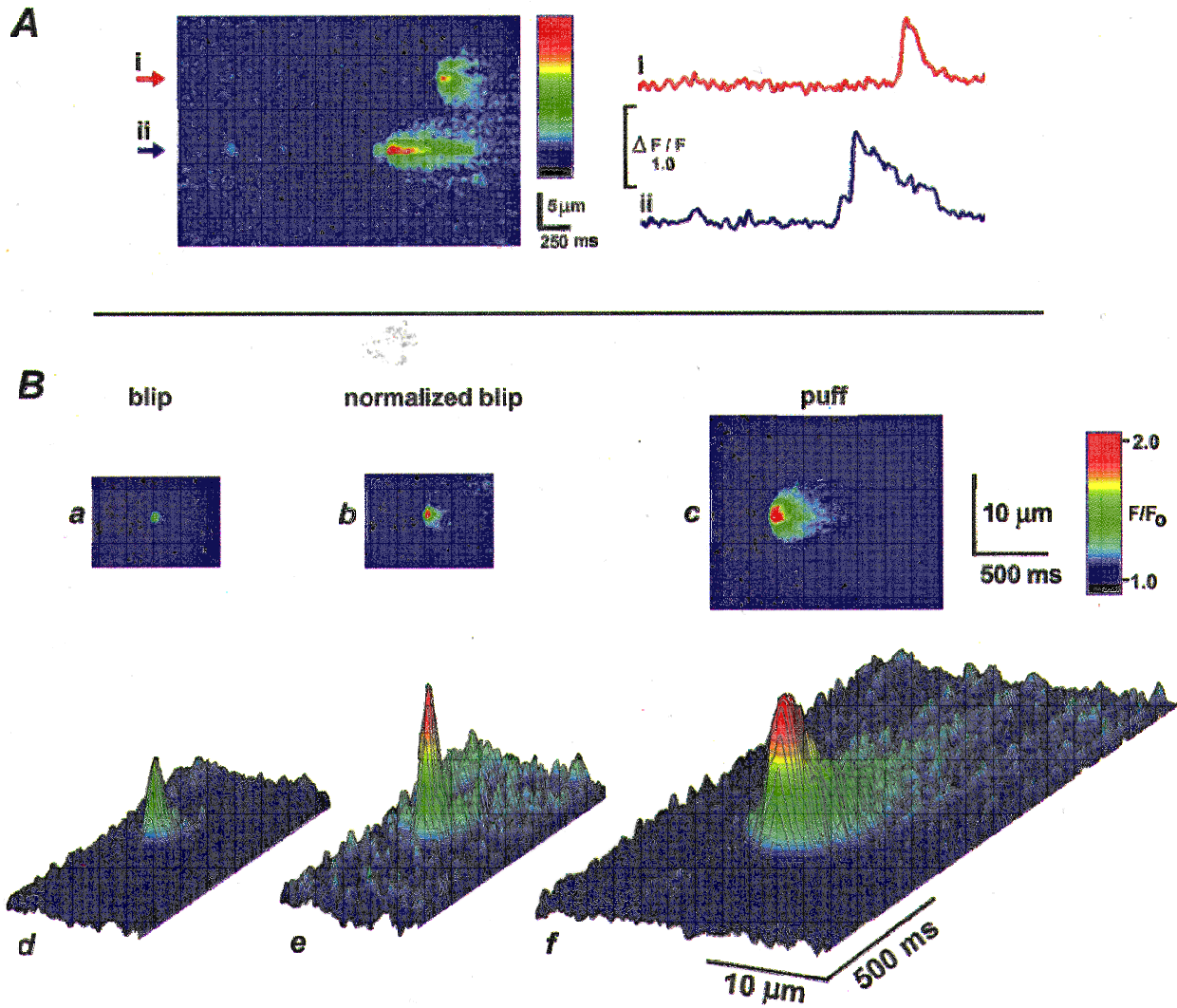


**Figure 3. Puffs and blips**

*A*, the linescan image on the left illustrates calcium events of differing magnitudes at 2 sites (i and ii). Both sites showed puffs and site ii showed, in addition, two much smaller events ('blips') – one in isolation near the start of the image, and a second immediately preceding the puff. The colour bar indicates  $F/F_0$  from 0.9 to 2.2. The photolysis flash occurred before the start of the image. Traces at the right show fluorescence signals monitored over 0.6 μm windows centered on the sites marked by arrowheads in the image. *B*, images showing averages of 4 selected small events (blips) and 5 large events (puffs) in the animal hemisphere of a single oocyte. Averages were obtained by aligning the times and positions of maximal fluorescence during each event. The upper panel (*a–c*) shows averages of blips (*a*) and puffs (*c*) with their fluorescence amplitudes depicted by the same colour scale, and (*b*) after normalizing the averaged blip to the same peak fluorescence intensity as the puff. The lower panel (*d–f*) shows the same data as *a–c*, but replotted as a surface representation where  $[Ca^{2+}]$  is coded both by colour and by height of the surface. The rise in fluorescence towards the end of the blip record is artifactual, and due to inclusion in the average of some instances where calcium from distant puffs diffused into the image frame.

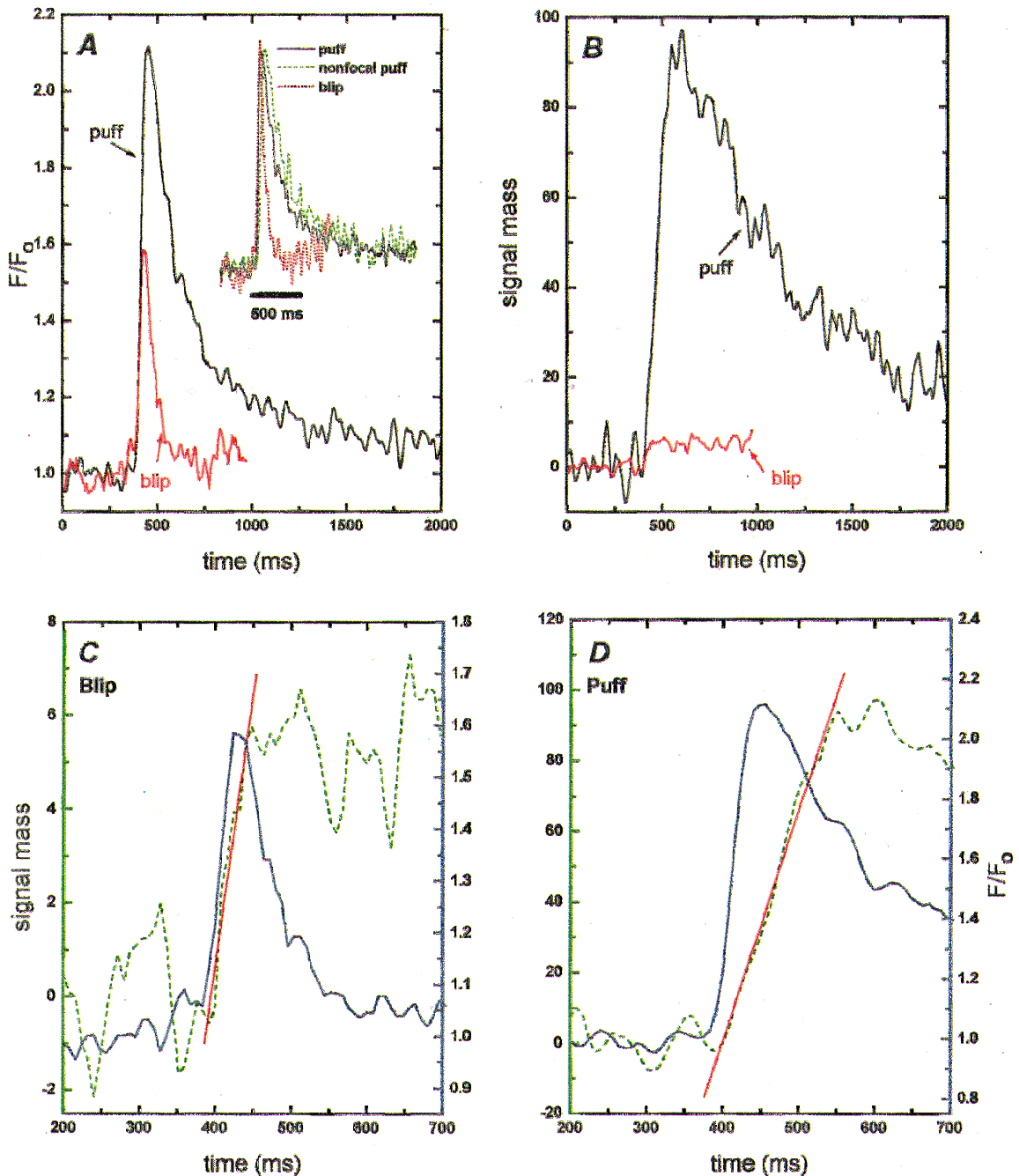


**Figure 4. Kinetics of peak fluorescence and signal mass during blips and puffs**

In *A*, the main panel shows time courses of fluorescence during the averaged puff (black trace) and blip (red trace) shown in Fig. 3*B*. Measurements were made averaging over a 3 pixel ( $0.4 \mu\text{m}$ ) window, centered at the position of maximum fluorescence. Inset shows the puff and blip normalized to the same peak height to facilitate comparison of their kinetics. The green trace shows normalized fluorescence during the puff monitored at a distance of  $2 \mu\text{m}$  from the release site, where the peak fluorescence signal matched the amplitude of the blip. *B*, time courses of signal mass (in units of  $\Delta F/F_0 \times 10^{-15}$ ) during the puff (black trace) and blip (red trace). *C* and *D*, kinetics of fluorescence signals (blue traces; right-hand scales expressed as  $F/F_0$ ) during the averaged blip (*C*) and puff (*D*), together with corresponding measurements of signal mass (green traces; left-hand scales expressed in units of  $\Delta F/F_0 \times 10^{-15}$ ). Note that scales of both ordinates differ between *C* and *D*. The continuous red lines are linear regressions fitted to the rising phases of the signal mass traces.

**Amounts of calcium liberated during elementary events**

Measurements of fluorescence intensity at a release site correspond to the local free calcium concentration at the confocal spot, but do not give a measure of the amount of calcium liberated during release events. Instead, we estimated this by calculating the ‘signal mass’ associated with release events (see Methods). The underlying assumption in this calculation is that for sharply resolved events, the laser scan line cuts through the centre of a spherically symmetrical ‘cloud’ of calcium diffusing from a point source of release. Fluorescence along the scan line then represents a profile of calcium across a diameter of this sphere, and the total fluorescence change associated with an event can be computed by integrating the profile throughout three dimensions. For convenience, we express the resulting signal mass in units of  $\Delta F/F_0 \times 10^{-15}$  l; that is to say, one signal mass unit corresponds to a doubling in fluorescence throughout a volume of 1 fl. Given that the intracellular dye concentration was about  $40 \mu M$ , and that injections of saturating amounts of calcium into the oocyte produced a maximal fluorescence increase ( $\Delta F/F_0$ ) of 4–5, then a signal of  $\Delta F/F_0 = 1$  corresponds to binding of about  $10 \mu M$  calcium to the indicator. We had previously estimated (Yao *et al.* 1995) that the amount of calcium bound to endogenous buffers would be approximately equal to that bound to the dye, and that the amount of free calcium is small in comparison to that bound. Thus, 1 signal mass unit would

correspond to roughly  $2 \times 10^{-20}$  moles (mol) of calcium ( $20 \mu M$  in a volume of 1 fl): equivalent to a calcium current of about 4 pA for 1 ms.

Figure 4 shows the time courses of fluorescence signals (A) and signal mass (B) for the averaged puff and blip images in Fig. 3B. A striking point is that although the peak fluorescence signals during the blip and puff differed only about 2-fold, the signal mass associated with the puff was more than 10 times greater, presumably because calcium flux occurred at a greater rate and for a longer time.

The kinetics of the fluorescence and signal mass records are shown on expanded time scales in Fig. 4C and D. During both the blip and the puff, the signal mass showed slower rising and falling phases as compared with the fluorescence signal. A slower falling phase is expected, because fluorescence measured directly at a release site will decline rapidly following termination of calcium liberation as calcium ions diffuse into the virtually infinite bulk of the oocyte, whereas diffusional spread of calcium should cause no change in signal mass provided that measurements are integrated throughout a sufficient volume (Yao *et al.* 1995). Instead, the decay of signal mass following termination of release will reflect factors (such as resequestration and extrusion from the cell) that remove calcium from the cytosol. Given that the decay of the signal mass is slow compared with its rise, the slope of the rising phase then approximates the rate of calcium flux into the cytosol, and

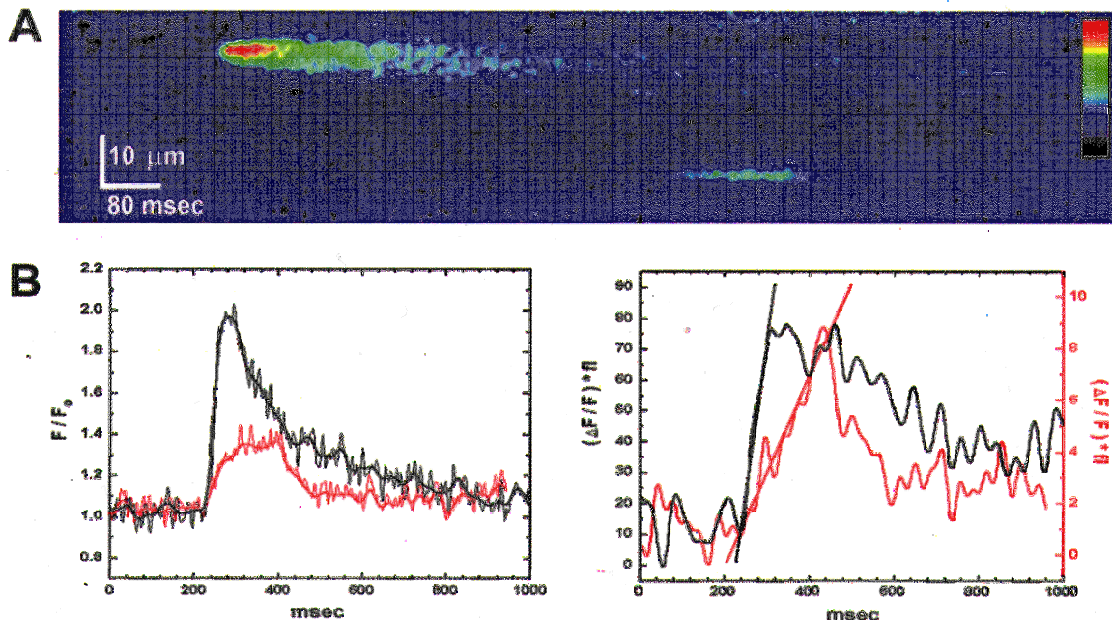


**Figure 5. Puff and sustained blip recorded with fast time resolution**

A, linescan image obtained at a scan rate of 1.5 ms per line, showing a puff (upper event) and a prolonged blip arising at adjacent release sites. B, time courses of fluorescence (left) and signal mass (right) during the puff (black) and blip (red). Note that ordinate scales for signal mass ( $1 \Delta F/F_0 \times 10^{-15}$  l) are different for the puff and the blip. Regression lines fitted to the rising phases of the signal mass traces have slopes of  $0.95 \text{ units ms}^{-1}$  (puff) and  $0.036 \text{ units ms}^{-1}$  (blip).

the peak value of the signal mass provides a measure of the total amount of calcium liberated.

From the calibration detailed above, the peak signal mass values during the averaged blip and puff in Fig. 4 correspond, respectively, to about  $1.2 \times 10^{-19}$  and  $2 \times 10^{-18}$  mol of calcium. The duration of the rising phase of the signal mass trace was clearly more prolonged during the puff as compared to the blip (Fig. 4C and D), indicating that more calcium was released because of an increased duration as well as an increased rate of release. The rates of rise of signal mass from these traces are about 0.1 and 0.62 signal mass units  $\text{ms}^{-1}$  for the blip and puff, respectively – corresponding to calcium fluxes of roughly  $2 \times 10^{-21}$  and  $1.2 \times 10^{-20}$  mol  $\text{ms}^{-1}$ , or calcium currents of roughly 0.4 and 2.5 pA. Finally, the slower time to peak of the signal mass trace in comparison with the fluorescence signal during the puff suggests that calcium liberation persists even while the fluorescence signal begins to decay.

### Prolonged blips

To determine if the low amplitude of blips with brief time courses (e.g. Figs 3 and 4) may have arisen artifactually through slow equilibration of the indicator or limited temporal resolution of the imaging (8 ms per line), we obtained recordings with improved time resolution (1.5 ms per line). Figure 5A shows an image that includes a puff at one site, and an unusually prolonged blip of smaller fluorescence amplitude arising at an adjacent site. The spatial spread of the blip was restricted, indicating that the recording was focal at the release site. In contrast to the rapid rise and roughly exponential fall of fluorescence during the puff, the fluorescence during the blip showed a maintained plateau at about one-third the peak level of the puff, lasting for approximately 150 ms (Fig. 5B). During this time, the signal mass increased almost linearly, to a peak level about one-tenth that of the puff (Fig. 5B), and the rates of rise of signal mass corresponded to estimated  $\text{Ca}^{2+}$  currents of 0.15 pA for the blip and 3.8 pA for the puff.

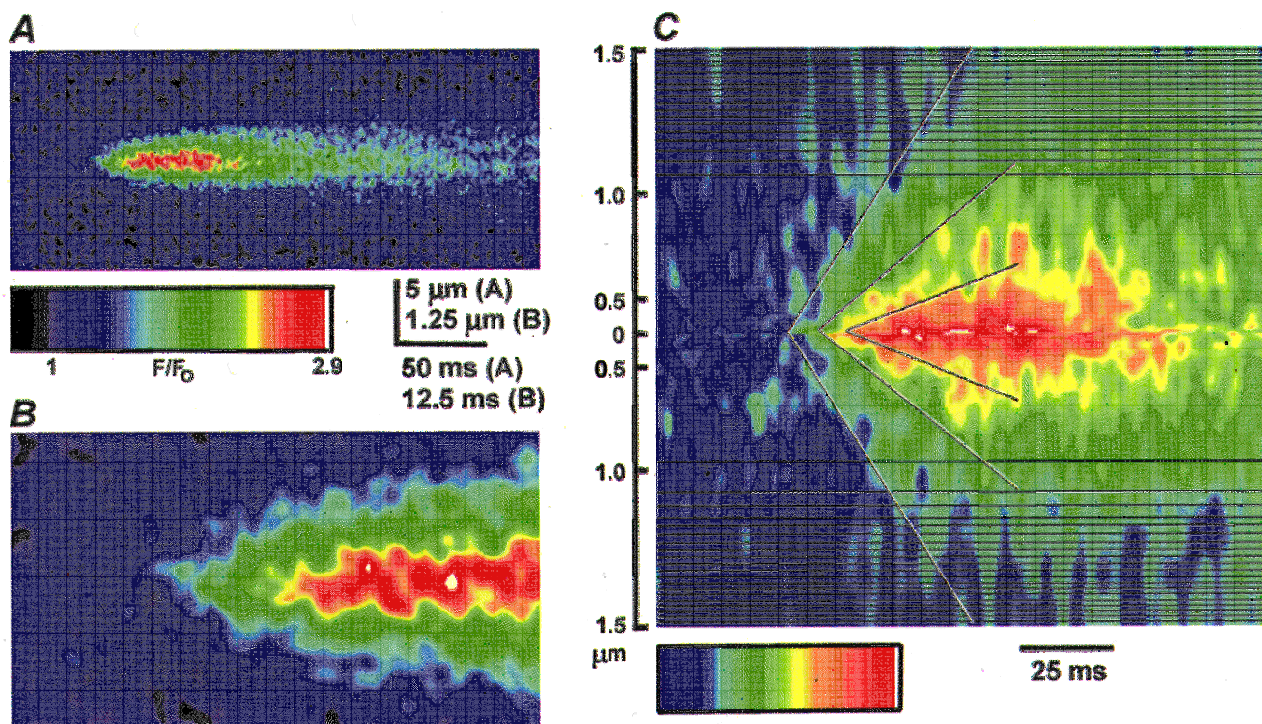


**Figure 6.** Spatial spread of calcium during a puff is consistent with liberation from a point source

A, image shows an average of 5 sharply focal puffs, recorded at a resolution of 1.5 ms per line and  $0.2 \mu\text{m}$  per pixel. The average was formed by aligning in time and space the first detectable rise in fluorescence during individual events. Individual images were re-binned by a factor of 2 in both axes, and then smoothed by a  $3 \times 3$  pixel window before averaging. B, expanded view of the rising phase of the averaged puff in A. C, the same event as in A, transformed so that the vertical axis depicts the square of the distance from the site of origin of the puff and depicted using a colour table adjusted to better emphasize contours of isofluorescence. Diffusive spread of calcium from a point origin is expected to progress linearly on this scale and the diagonal lines are drawn by eye through contours of equal fluorescence intensity during the rising phase of the puff. The horizontal black lines in the image are an artifact of the algorithm used to generate the transform.

It is clear, therefore, that events involving release of very small amounts of calcium may arise through sustained flux at a low rate, as well as through release which terminates rapidly.

**Puffs involve calcium liberation from a ‘point’ source**

We have previously suggested that puffs arise through calcium liberation from a virtual point source of release (< 1 μm across), rather than involving InsP<sub>3</sub>R distributed throughout an appreciable region (Yao *et al.* 1995). Different from this, Bootman *et al.* (1997*b*) describe an instance where a puff appears to arise through a microscopic calcium wave within a puff site. We were thus interested in reinvestigating the spatial distribution of calcium during puffs in the oocyte, taking advantage of the improved resolution provided by our current confocal microscope. This issue is important not only for the information it provides about the morphological arrangement of functional calcium release channels, but because the procedure described above for estimation of signal mass depends on an assumption of calcium originating from a point source.

Figure 6*A* shows an averaged image of five puffs that were selected as being of roughly uniform size, sharply focused, and involving only a single release site. An enlarged view of the beginning of the averaged puff (Fig. 6*B*) shows that calcium release began at a site with an apparent width of approximately 0.25 μm (i.e. at the limit of resolution of the microscope), and then spread over a radial distance of about 2 μm. From Fick’s law, the mean distance calcium ions diffuse from a point of release increases proportionally to

the square root of time (Hille, 1992). To examine whether passive diffusion accounts for the spatiotemporal distribution of calcium during the puff, we transformed the linescan image so that the vertical axis depicted displacement from the puff origin on a scale of distance squared (Fig. 6*C*). Following this transformation, contours of iso-fluorescence (i.e. equal free [Ca<sup>2+</sup>]) extended approximately linearly with time, consistent with diffusion from a point source. Thus, within the limits set by optical microscopy, it appears that the puff can be considered as arising through calcium diffusing from a point source, rather than involving a propagating ‘micro-wave’.

**Blips and puffs arise at the same sites**

We had originally proposed that puffs and blips both arose from release sites comprising a tight cluster of several InsP<sub>3</sub>R channels, but that whereas puffs may involve near-synchronous activation of many channels, blips may arise through openings of only one, or a few, channels within a cluster (Parker & Yao, 1996; Parker *et al.* 1996*a*). Those studies, however, utilized a stationary point confocal fluorimeter that did not provide spatial information, so an alternative possibility was that blips may arise from isolated channels present at a low density between the clusters of channels at puff sites. It was thus important to determine, using linescan imaging, whether sites of blips and puffs co-localize.

Images such as that in Fig. 3*A* already indicated that blips were observed at the same sites as puffs, and Fig. 7 presents a more detailed analysis from an experiment in which records

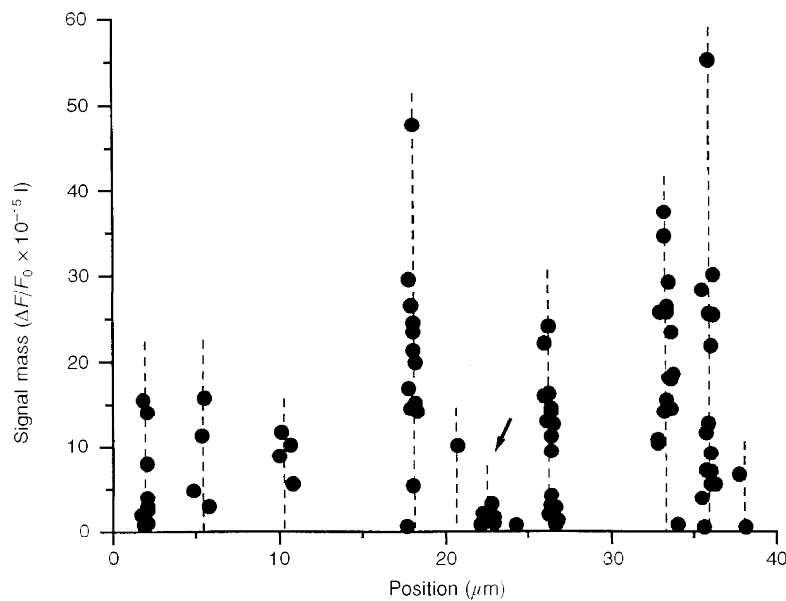


**Figure 7. Individual release sites generate events involving widely varying amounts of calcium**

The scatter plot shows estimated amounts of calcium liberation (signal mass) during events occurring at 11 discrete locations (indicated by dashed vertical lines) along a fixed scan line. Data from 86 individual events are included, measured from 23 linescan images at a fixed point in response to identical photolysis flashes.

were made from a fixed scan line in response to twenty-three successive, identical photolysis flashes. Measurements were made of the signal mass associated with all sharply resolved release events, and are plotted against the location of each event. The data fall into tight groups at particular locations (indicated by dashed lines) along the scan line,

indicating that events recurred at sites that remained fixed during the 20 min recording period, and that release sites could be located reproducibly to within about  $0.5 \mu\text{m}$ . Several of the sites showed a range of events with widely varying magnitudes. Further, the tight co-localization of small and large events at these sites, together with the relatively large

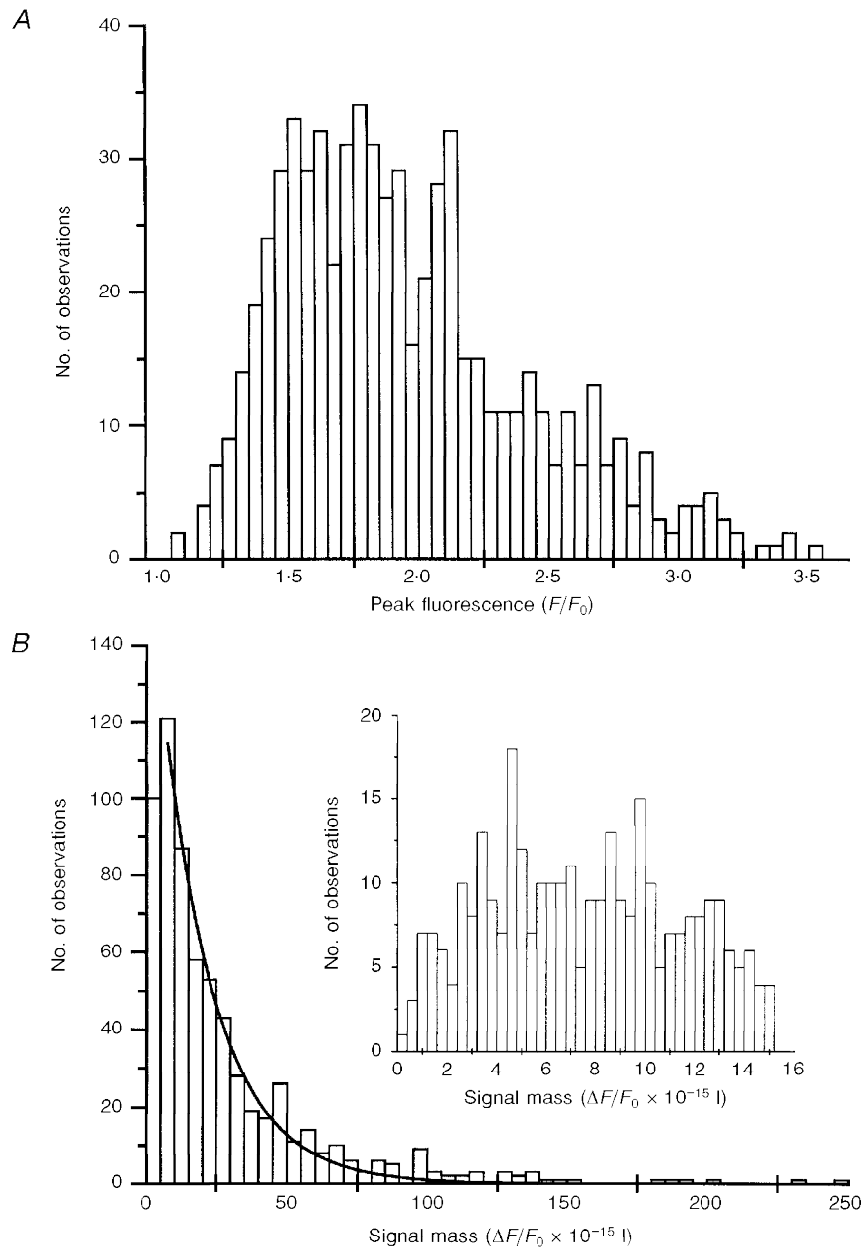


**Figure 8.** Distributions of peak fluorescence signals and amounts of calcium liberated during elementary events

Data are derived from a total of 655 elementary calcium signals (puffs and blips) recorded at  $>100$  sites in the animal hemispheres of 12 oocytes. Events judged to involve synchronous release at 2 or more sites were excluded. *A*, histogram showing distribution of peak fluorescence signals ( $F/F_0$ ) during events. *B*, distribution of peak signal mass associated with the same events. One unit on the abscissa corresponds to a doubling of fluorescence (i.e.  $\Delta F/F_0 = 1$ ) throughout a volume of 1 fl. The inset shows the distribution of small events on an expanded scale.

spacing between sites (mean spacing about  $4 \mu\text{m}$ ), makes it unlikely that this arose because discrete blip sites happened, coincidentally, to be located close to puff sites. We thus conclude that a given calcium release site can generate both puffs and blips, though it remains possible that certain sites (see arrow in Fig. 7) generate preponderantly small events.

The data in Fig. 7 also demonstrate a wide variation in the numbers of events observed at specific sites, with some locations showing as many as thirteen to sixteen events and others as few as one or two. This is unlikely to have arisen through a variation in the extent of photorelease of  $\text{InsP}_3$  across the scan line, since 'infrequent' sites were observed close to 'frequent' sites. Instead, the differences in event frequency may reflect differences in sensitivities to  $\text{InsP}_3$ . In earlier experiments, using localized photorelease of  $\text{InsP}_3$  to assess the sensitivities of separate sites, we had failed to resolve such heterogeneity (Parker *et al.* 1996a) but, as a result of the steep power relationship between puff occurrence and  $[\text{InsP}_3]$  (Callamaras *et al.* 1998), only small differences in sensitivity may be sufficient to account for the observed variation in the occurrence of events.

#### Blips and puffs represent opposite ends of a continuum of release events

The distribution of peak fluorescence signals, measured from a total of 655 events (blips and puffs) is plotted in Fig. 8A. This shows a skewed distribution over a roughly 5-fold range of magnitudes, with a peak of smaller events ( $F/F_0$ ) at approximately 1.5, and an extended 'tail' of events with progressively larger amplitudes up to a maximum of about  $3.5 F/F_0$ . The data are clearly not consistent with a Gaussian distribution of a single population of events, but they also do not reveal two discrete populations of events of differing amplitudes, as we had previously proposed on the basis of more limited measurements (Parker & Yao, 1996). Rather than arising through discrete events, blips and puffs appear to represent opposite ends of a continuous distribution.

This conclusion is further strengthened by the distribution of amounts of signal mass associated with each event (Fig. 8B). The distribution differs markedly from that of the peak fluorescence, and encompasses a much greater range (100-fold or more) between the largest and smallest discernible events. The main plot in Fig. 8B shows signal mass measurements from the same events as in Fig. 8A. This follows a continuous, exponential distribution, with progressively fewer larger events and an overall mean of 19.4 signal mass units (about  $4 \times 10^{-19}$  mol calcium). The inset shows the distribution of smaller events on an expanded scale. There is a fall-off in numbers of observed events with signal mass values below about five, but this probably resulted from a failure to resolve very small fluorescence signals above the noise level. The smallest signals that could reliably be discerned had a signal mass of about one, corresponding to about  $2 \times 10^{-20}$  mol calcium.

## DISCUSSION

### A continuum of elementary calcium signals

Previous work has shown that global  $\text{InsP}_3$ -mediated calcium signals can be devolved into elementary units, characterized as transient, localized  $\text{Ca}^{2+}$  release events (Parker & Yao, 1991; Yao *et al.* 1995; Parker *et al.* 1996a; Thorn, 1996; Bootman *et al.* 1997b). Further, observations of signals of differing magnitudes suggested a hierarchy of calcium signalling events, with the smaller blips representing 'fundamental' events involving opening of single  $\text{InsP}_3\text{R}$  channels and the larger puffs being 'elementary' events resulting from the concerted opening of small groups of  $\text{InsP}_3\text{Rs}$  (Parker & Yao, 1996; Parker *et al.* 1996a; Lipp & Niggli, 1996; Bootman *et al.* 1997b; Berridge, 1997). The present results confirm that  $\text{InsP}_3$ -mediated calcium release is confined to specific subcellular sites that give rise to transient, localized signals. The improved spatial and temporal resolution provided by the linescan confocal microscope used in the present study reveals, however, that calcium liberation is not functionally quantized into discrete, stereotypical events of clearly separable magnitude as proposed earlier. Instead, the amounts of calcium liberated during different events show a continuous distribution over a wide range, even when monitored from a single site.

We thus find no clear distinction between 'fundamental' and 'elementary' events but, instead, propose that localized calcium liberation varies in a continuous fashion due to stochastic variation in both numbers of channels recruited and durations of channel openings. Furthermore, the spatio-temporal distribution of calcium during puffs is consistent with flux from a 'point' source with dimensions smaller than the resolution of an optical microscope (Fig. 6). Both puffs and blips therefore probably involve recruitment of varying numbers of channels within a tight cluster of  $\text{InsP}_3\text{R}$ , across which  $[\text{Ca}^{2+}]$  will equilibrate on a sub-millisecond time scale.

A similar continuum of elementary calcium signalling events is also observed in HeLa cells. In a paper published after submission of this manuscript, Bootman, Berridge & Lipp (1997a) describe elementary signals with variable amplitudes originating from a common point source, and conclude that this arises because variable numbers of  $\text{InsP}_3\text{R}$  can be recruited within a cluster.

To clarify the nomenclature, we use the generic term 'elementary event' to refer to any transient, localized calcium signal irrespective of how many channels may be involved, but continue to use the terms blips and puffs to refer in a qualitative manner to relatively small and large local  $\text{InsP}_3$ -evoked signals.

### Amounts of calcium liberated during elementary calcium signals

The continuum of event sizes probably arises because the release events involve only individual or small numbers of channels, so that their characteristics are determined by

stochastic channel gating rather than reflecting the mean behaviour of large populations of channels. Thus, analogous to the wide variability in lifetime of individual openings of a muscle endplate channel as compared with the consistent time course of endplate currents involving thousands of channels (Hille, 1992), individual calcium release events vary widely in magnitude and kinetics in comparison to the highly reproducible global calcium waves. The rate of rise of fluorescence signal mass during small but clearly resolved blips corresponds to an estimated calcium flux of  $2 \times 10^{-21}$  mol  $\text{ms}^{-1}$ , or a current of  $< 0.5$  pA. Although this value should be regarded as only approximate, and depends upon uncertain assumptions regarding calcium buffering in the cell, it is consistent with estimates of calcium current through a unitary  $\text{InsP}_3\text{R}$  under physiological conditions (about 0.5 pA; Callamaras & Parker, 1994; Bezprozvanny & Ehrlich, 1994). The much greater total liberation of calcium during larger puffs appears to involve both recruitment of additional channels and prolongation of the release process. The estimated calcium flux corresponds to currents of around 2.5 pA, and persists at least 4 times longer than during blips, thus accounting for the 20-fold or greater total amounts of calcium released. If the single channel current is taken to be 0.5 pA and the calcium current underlying the puff to be 2.5 pA, this yields a minimum estimate for the number of channels in a release site of five. Given the considerable uncertainties in computing calcium currents associated with puffs and single channels, this figure is close to the maximum number ( $\sim 8$ ) of  $\text{InsP}_3\text{R}$  channels observed in multi-channel patches from *Xenopus* nuclei (Mak & Foskett, 1997), suggesting a similar clustered organization of  $\text{InsP}_3\text{R}$  in the nuclear envelope and endoplasmic reticulum of oocytes.

We had previously estimated calcium currents underlying puffs to be 11–23 pA based on similar assumptions regarding calcium buffering and dye properties (Yao *et al.* 1995). The smaller value obtained here arises, in part, because the signal mass measurements indicate that flux occurs for  $> 100$  ms, rather than for about 50 ms, as we had earlier estimated from the rising phase of the fluorescence signal. Also, the poorer resolution of our earlier system may have biased the size of events selected for analysis.

#### Kinetics of calcium flux during elementary events

The generation of elementary calcium events must involve excitatory and inhibitory processes acting locally at the release site to initiate and terminate calcium liberation. Confocal imaging provides a unique opportunity to characterize these behaviours of the  $\text{InsP}_3$  receptor at the level of individual channels within an intact cell. Interpretation of the imaging data is, however, not straightforward.

A convenient starting point is to consider the free calcium concentration close to the mouth of a channel releasing calcium into the cytosol. This will rise almost instantly

(within microseconds) to a very high, steady value upon opening of the channel and then subside with similar rapidity to the resting level when the channel closes (Stern, 1992). Fluorescence recordings made using a 'perfect' indicator and monitored from an infinitely small point at the channel mouth will then directly reflect these free calcium changes. On the other hand, measurements of fluorescence throughout a volume around the channel sufficiently large to encompass diffusing  $\text{Ca}^{2+}$  ions will represent an integral of the net calcium flux; that is to say, the signal will rise at a rate roughly proportional to the calcium current while the channel is open, and will decline slowly after the channel closes as calcium is removed from the cytosol by various means. Our confocal recordings appear to fall somewhere between these two extremes, due to factors including the finite volume of the confocal spot and the kinetics of binding of calcium to the indicator (Parker *et al.* 1996). Nevertheless, the ability of the microscope to resolve transients rising as rapidly as 2–3 ms during calcium sparks in cardiac myocytes (W. G. Wier & I. Parker, unpublished data) and during ionophoretic calcium pulses (I. Parker, unpublished data) indicates that focal fluorescence signals report a stepwise onset of calcium flux with a lag of only a few milliseconds. The relatively slow rise of fluorescence during puffs (*ca* 50 ms) does not, therefore, arise artifactually through limitations of the indicator or of instrumentation, but must reflect a progressive increase in calcium conductance. Further, the signal mass (cumulative amount of calcium released) continues to rise for about 50 ms after the local fluorescence signal reaches a peak (Fig. 4), suggesting that calcium flux persists for some time after the fluorescence has begun to decline. Fluorescence measurements close to the release site appear, therefore, to correspond more closely to the rate of calcium flux as opposed to its integral. The peak fluorescence thus corresponds to the time when flux is maximal, rather than to the time when calcium liberation ceases.

Spontaneous opening of an  $\text{InsP}_3$ -bound receptor channel resulting from stochastic binding of calcium ion(s) may serve to initiate a puff. The net calcium flux from the release site then increases over tens of milliseconds as further channels are recruited and/or the open probability of individual channels progressively increases due to positive feedback by CICR (Iino, 1990; Bezprozvanny *et al.* 1991; Finch *et al.* 1991). The rate of regenerative activation during the rising phase of the puff is much slower than during sparks in cardiac muscle (Cheng *et al.* 1993), suggesting that the kinetics of calcium activation of  $\text{InsP}_3\text{R}$  in the oocyte are slower than those of cardiac RyR. Subsequent termination of calcium liberation is unlikely to be attributable to local depletion of stores (Golovina & Blaustein, 1997), as this mechanism is expected to give rise to events of uniform magnitude and is difficult to reconcile with the variability in event durations. More likely,  $\text{InsP}_3\text{R}$  channels enter an inactivated closed state, and the exponential distributions of

event durations and amounts of calcium liberation are consistent with this being a stochastic process. Feedback by  $\text{Ca}^{2+}$  ions binding to an inhibitory site on the  $\text{InsP}_3\text{R}$  is well established (Bezprozvanny *et al.* 1991; Finch *et al.* 1991), but more recent experiments suggest that the major factor determining the termination of calcium release is an obligatory intrinsic inactivation of the calcium-sensitized state of the  $\text{InsP}_3\text{R}$  (Ilyin & Parker, 1994; Hajnoczky & Thomas, 1997).

- BERRIDGE, M. J. (1993). Inositol trisphosphate and calcium signalling. *Nature* **361**, 315–325.
- BERRIDGE, M. J. (1997). Elementary and global aspects of calcium signalling. *Journal of Physiology* **499**, 291–306.
- BEZPROZVANNY, I. & EHRLICH, B. E. (1994). Inositol (1,4,5)-trisphosphate ( $\text{InsP}_3$ )-gated  $\text{Ca}^{2+}$  channels from cerebellum: conduction properties for divalent cations and regulation by intraluminal calcium. *Journal of General Physiology* **104**, 821–856.
- BEZPROZVANNY, I., WATRAS, J. & EHRLICH, B. E. (1991). Bell-shaped calcium-response curves for  $\text{Ins}(1,4,5)\text{P}_3$ - and calcium-gated channels from endoplasmic reticulum of cerebellum. *Nature* **351**, 751–754.
- BOOTMAN, M. D. (1994). Questions about quantal  $\text{Ca}^{2+}$  release. *Current Biology* **4**, 169–172.
- BOOTMAN, M. D., BERRIDGE, M. J. & LIPP, P. (1997a). Cooking with calcium; the recipes for composing global calcium signals from elementary events. *Cell* **91**, 367–373.
- BOOTMAN, M. D., NIGGLI, E., BERRIDGE, M. J. & LIPP, P. (1997b). Imaging the hierarchical  $\text{Ca}^{2+}$  signalling system in HeLa cells. *Journal of Physiology* **499**, 307–314.
- CALLAMARAS, N., MARCHANT, J. S., SUN, X.-P. & PARKER, I. (1998). Activation and co-ordination of  $\text{InsP}_3$ -mediated elementary  $\text{Ca}^{2+}$  events during global  $\text{Ca}^{2+}$  signals in *Xenopus* oocytes. *Journal of Physiology* **509**, 81–91.
- CALLAMARAS, N. & PARKER, I. (1994). Inositol 1,4,5-trisphosphate receptors in *Xenopus laevis* oocytes: localization and modulation by calcium. *Cell Calcium* **15**, 60–72.
- CALLAMARAS, N. & PARKER, I. (1998). Caged inositol 1,4,5-trisphosphate for studying release of  $\text{Ca}^{2+}$  from intracellular stores. *Methods in Enzymology* **291**, 380–403.
- CHENG, H., LEDERER, W. J. & CANNELL, M. B. (1993). Calcium sparks – elementary events underlying excitation–contraction coupling in heart muscle. *Science* **262**, 740–744.
- FABIATO, A. (1985). Simulated calcium current can both cause calcium loading and trigger calcium release from sarcoplasmic reticulum of a skinned canine cardiac Purkinje cell. *Journal of General Physiology* **85**, 291–320.
- FINCH, E. A., TURNER, T. J. & GOLDIN, S. M. (1991). Calcium as a coagonist of inositol 1,4,5-trisphosphate-induced calcium release. *Science* **252**, 443–446.
- GOLOVINA, V. A. & BLAUSTEIN, M. P. (1997). Spatially and functionally distinct  $\text{Ca}^{2+}$  stores in sarcoplasmic and endoplasmic reticulum. *Science* **275**, 1643–1648.
- HAJNOCZKY, G. & THOMAS, A. P. (1997). Minimal requirements for calcium oscillations driven by the  $\text{IP}_3$  receptor. *EMBO Journal* **16**, 3533–3543.
- HILLE, B. (1992). *Ionic Channels of Excitable Membranes*. Sinauer Associates, Sunderland, MA, USA.
- IINO, M. (1990). Biphasic calcium dependence of inositol 1,4,5-trisphosphate-induced calcium release in smooth muscle cells of the guinea pig taenia caeci. *Journal of General Physiology* **95**, 1103–1122.
- ILYIN, V. & PARKER, I. (1994). Role of cytosolic  $\text{Ca}^{2+}$  in inhibition of  $\text{InsP}_3$ -evoked  $\text{Ca}^{2+}$  release in *Xenopus* oocytes. *Journal of Physiology* **477**, 503–509.
- KLEIN, M. G., CHENG, H., SANTANA, L. F., JIANG, Y.-H., LEDERER, W. J. & SCHNEIDER, M. F. (1996). Two mechanisms of quantized calcium release in muscle. *Nature* **379**, 455–458.
- LECHLEITER, J. D. & CLAPHAM, D. E. (1992). Molecular mechanisms of intracellular calcium excitability in *X. laevis* oocytes. *Cell* **69**, 283–294.
- LIPP, P. & NIGGLI, E. (1996a). Submicroscopic calcium signals as fundamental events of excitation–contraction coupling in guinea-pig cardiac myocytes. *Journal of Physiology* **492**, 31–38.
- LIPP, P. & NIGGLI, E. (1996b). A hierarchical concept of cellular and subcellular  $\text{Ca}^{2+}$  signalling. *Progress in Biophysics and Molecular Biology* **65**, 265–296.
- LOPÉZ-LOPÉZ, J. R., SHACKLOCK, P. S., BALKE, C. W. & WIER, W. G. (1995). Local calcium transients triggered by single L-type calcium channel currents in cardiac cells. *Science* **268**, 1042–1045.
- MAK, D.-O. D. & FOSKETT, J. K. (1997). Single channel kinetics, inactivation, and spatial distribution of inositol trisphosphate ( $\text{IP}_3$ ) in *Xenopus* oocyte nucleus. *Journal of General Physiology* **109**, 571–587.
- MARCHANT, J. S., CALLAMARAS, N., SUN, X.-P. & PARKER, I. (1998). A continuum of subcellular  $\text{Ca}^{2+}$  signals in the *Xenopus laevis* oocyte. *Journal of Physiology* **506.P**, 70P.
- NELSON, M. T., CHENG, H., RUBART, M., SANTANA, L. F., BONEY, A. D., KNOT, H. & LEDERER, W. J. (1995). Relaxation of arterial smooth muscle by calcium sparks. *Science* **270**, 633–637.
- PARKER, I. (1992). Use of caged intracellular messengers for studying the inositol trisphosphate pathway. In *Neuromethods*, vol. 20, *Intracellular Messengers*, ed. BOULTON, A. A., BAKER, G. B. & TAYLOR, C. W., pp. 369–393. Humana Press, Totowa, NJ, USA.
- PARKER, I., CALLAMARAS, N. & WIER, W. G. (1997). A high resolution confocal laser scanning microscope and flash photolysis system for physiological studies. *Cell Calcium* **21**, 441–452.
- PARKER, I., CHOI, J. & YAO, Y. (1996a). Elementary events of  $\text{InsP}_3$ -induced  $\text{Ca}^{2+}$  liberation in *Xenopus* oocytes: hot spots, puffs and blips. *Cell Calcium* **20**, 105–121.
- PARKER, I. & IVORRA, I. (1990). Inhibition by  $\text{Ca}^{2+}$  of inositol-trisphosphate-mediated  $\text{Ca}^{2+}$  liberation: A possible mechanism for oscillatory release of  $\text{Ca}^{2+}$ . *Proceedings of the National Academy of Sciences of the USA* **87**, 260–264.
- PARKER, I. & YAO, Y. (1991). Regenerative release of calcium from functionally discrete subcellular stores by inositol trisphosphate. *Proceedings of the Royal Society B* **246**, 269–274.
- PARKER, I. & YAO, Y. (1996).  $\text{Ca}^{2+}$  transients associated with openings of inositol trisphosphate-gated channels in *Xenopus* oocytes. *Journal of Physiology* **491**, 663–668.
- PARKER, I., ZANG, W.-J. & WIER, W. G. (1996b).  $\text{Ca}^{2+}$  sparks involving multiple  $\text{Ca}^{2+}$  release sites along Z-lines in rat heart cells. *Journal of Physiology* **497**, 31–38.
- STERN, M. D. (1992). Buffering of calcium in the vicinity of a channel pore. *Cell Calcium* **13**, 183–192.

- SUN, X.-P., CALLAMARAS, N. & PARKER, I. (1997). A continuum of calcium signaling events in *Xenopus* oocytes. *Society for Neuroscience Abstracts* **23**, 705.
- TAKAMATSU, T. & WIER, W. G. (1990). Calcium waves in mammalian heart: Quantification of origin, magnitude, waveform and velocity. *Federation Proceedings* **4**, 1519–1525.
- TAYLOR, C. W. & TRAYNOR, D. (1995). Calcium and inositol trisphosphate receptors. *Journal of Membrane Biology* **145**, 109–118.
- THORN, P. (1966). Spatial domains of  $\text{Ca}^{2+}$  signaling in secretory epithelial cells. *Cell Calcium* **20**, 203–214.
- TSUGORKA, A., RIOS, E. & BLATTER, L. A. (1995). Imaging the elementary aspects of calcium release in skeletal muscle. *Science* **269**, 1723–1726.
- WIER, W. G., EGAN, T. M., LOPÉZ-LOPÉZ, J. R. & BALKE, C. W. (1994). Local control of excitation–contraction coupling in rat heart cells. *Journal of Physiology* **474**, 463–471.
- YAO, Y., CHOI, J. & PARKER, I. (1995). Quantal puffs of intracellular  $\text{Ca}^{2+}$  evoked by inositol trisphosphate in *Xenopus* oocytes. *Journal of Physiology* **482**, 533–553.

#### Acknowledgements

This work was supported by a grant (GM 48071) from the National Institutes of Health, and by a Wellcome Trust Prize Fellowship to J.S.M.

#### Corresponding author

I. Parker: Laboratory of Cellular and Molecular Neurobiology, Department of Psychobiology, University of California Irvine, Irvine, CA 92697-4550, USA.

Email: iparker@uci.edu

#### Authors' present addresses

X.-P. Sun: Department of Physiology, UCLA School of Medicine, Jerry Lewis Neuromuscular Research Center, Los Angeles, CA 90024, USA.

J. S. Marchant: Department of Pharmacology, University of Cambridge, Tennis Court Road, Cambridge CB2 1QJ, UK.